

Intraocular Lens Far Peripheral Vision: Image Detail and Negative Dysphotopsia

Michael J. Simpson, Ph.D.

Simpson Optics LLC, Arlington, TX 76012, USA

This work has no public or private financial support.

The authors have no financial or proprietary interest in anything discussed in the paper.

Presented in part at ARVO, Vancouver, Canada, April, 2019, and at the ESCRS, Paris, France, September 2019.

Corresponding author:

Michael J. Simpson, Ph.D.

Simpson Optics LLC,

3004 Waterway Ct, Arlington, TX 76012

USA.

This is the submitted author version of the paper published as:

Simpson MJ. Intraocular Lens Far Peripheral Vision: Image Detail and Negative Dysphotopsia. J Cataract Refract Surg 46:451-458 (2020).

Abstract

Purpose: To evaluate negative dysphotopsia in the far periphery of the pseudophakic eye by generating simulated images of text charts.

Setting: Consultancy.

Design: Laboratory study.

Methods: Simulated images of a peripheral text chart were created using a raytrace model of a pseudophakic eye. The point spread function (PSF) varies strongly with radial location. Retinal angles subtended at the 2nd nodal point were used to linearly scale retinal locations to a polar plot in object space, weighting rays by the object luminance, total transmittance, and a cosine normalization for pupil effects. Improved scaling using a phakic 70 year old eye was also explored.

Results: Images demonstrate a distinct shadow with a 2.5 mm pupil between the upper limit of the text image formed by the lens and a second larger image due to light missing the IOL. The shadow is rapidly softened by a small increase in pupil diameter.

Conclusions: The images verify characteristics that have been previously only inferred indirectly: (a) With a 2.5 mm pupil there is a prominent dark shadow. (b) Light missing the IOL experiences lower power and forms a larger image, and also comes from a lower visual angle. (c) A small increase in pupil diameter causes the shadow to fade. The calculations show that imaging in the far periphery is very different for the pseudophakic eye in comparison to the phakic eye. The limit of the focused image is probably the primary cause of the shadow yet relatively few patients find this to be bothersome.

INTRODUCTION

Hundreds of millions of patients have received intraocular lenses (IOLs) during cataract surgery, and there has rarely been any concern about the quality of vision in the far periphery. However, starting around the year 2000, patients occasionally reported bothersome dark shadows in their temporal peripheral visual field ¹. Since then there have been many publications about this type of “negative dysphotopsia” (ND), with the more recent ones summarizing the earlier papers²⁻⁶. Initially it was thought that these reports might be linked to specific intraocular lenses (IOLs) that had a high refractive index, but further evaluation found that the phenomenon was present with other lens materials also. Various potential causes were proposed, such as a visual phenomenon from the surgical incision, light passing through the edge of the IOL, and effects from the capsulorrhexis. Reports of cases that are particularly bothersome have been relatively rare, though 3 % may still see shadows at 1 year after surgery⁷, and a recent study identified over 1% of about 6,000 procedures as having ND ⁸.

Something that was not perhaps fully discussed initially was a comparison between the phakic lens and the IOL. These are depicted in Figure 1 as an overlay of preoperative and postoperative OCT images for the same eye, where the crystalline lens and IOL profiles are also identified. Preoperatively, all the light that enters the pupil is directed towards the same general region of the retina, even if the image is defocused and aberrated. Postoperatively, however, the IOL is physically very different. Using raytracing to evaluate an IOL in a model eye (Figure 2), it is found that at large visual angles, with a small pupil, the light no longer passes through an IOL at all because it is much smaller than the natural crystalline lens. The main image goes totally dark, and this is highly likely to be the primary cause of the shadow. This property of an optical system is called “vignetting” for a conventional lens, leading to a darkened periphery in early

camera images that had simple lenses. The thing that makes it bothersome for an IOL patient may be the fact that light can also bypass the IOL and illuminate the retina further out. This can leave a distinct shadow within an illuminated region of retina. The calculations also demonstrate that the shadow that is present with a small pupil is eliminated as the pupil opens up, which agrees with clinical reports. Evaluations of iris characteristics indicate that the typical gap between the posterior iris and the IOL is about 0.5 mm⁹⁻¹¹.

The visual angle at which the shadow is seen has not been usually recorded objectively, but a typical example is where a hand raised to the side of the face like a military salute will remove the effect. This indicates that it is caused by light at very large visual angles, and a recent paper gives a typical value of about 90°⁸. It is also always in the temporal direction, with the nose, eyebrow, and cheek blocking light from angles above about 60 degrees anyway. The large angle is consistent with the first reports of ND appearing about 20 years ago, when clearer peripheral capsules became more routine following the introduction of phacoemulsification, small incisions, and foldable IOLs with a sharp posterior edge. These improvements permitted light that had previously been obstructed or scattered when it missed the IOL to reach the retina directly.

It has only recently become clear quite how limited the scientific evaluation has been of the entire visual region of the far periphery¹². Perimetry is widely used to evaluate peripheral vision, but it is rarely used at large angles, and its purpose is primarily to assist with diagnosing specific diseases, rather than to characterize vision itself. Perimetry primarily relates input light sources to patient responses, and it is possible that the image on the retina during a perimetry test has never been modeled using raytracing. This type of modeling is actually difficult to do because

the image surface is highly curved. Even the latest raytrace software that is used here does not include standard tools to evaluate this.

Drawings of rays passing through the pseudophakic eye in the periphery all show the type of bifurcation that is depicted in Figure 2, using several calculation methods^{2,3,13,14}. The image formed in this region has to be different to that of the phakic eye, even though that is rarely noted (though image quality in the periphery is also extremely poor). These drawings have also been somewhat misleading, however, because although a single input beam splits into two when light starts missing the lens, the light that is seen in the periphery no longer comes from the largest visual angles because it does not experience the focusing power of the lens. The peripheral light hits the retina directly, and although it might “appear” to come from a larger angle because of its retinal location, the raytrace calculations indicate that the maximum visual field angle is reduced with an IOL.

More recent evaluations calculated illumination on the retina from an extended bright source, rather than just single rays^{15,16}. These were presented as retinal images transferred back to object space, by comparing retinal locations to object locations for the phakic eye using an initial estimate for the scaling. This method is now extended here to use an input text object, which evaluates the imaging properties from an enhanced perspective. A matching phakic eye model was also developed, as an initial attempt to compare the image properties between the phakic and pseudophakic eyes, with an improved estimate for the image scaling.

METHODS

The Zemax Optic Studio optical design software (Radiant Zemax, Redmond, WA) was used to generate raytrace data using an optical model for an average eye³. This has a 2.5 mm diameter

pupil (3.0 mm “apparent pupil”) decentered nasally by 0.25 mm. Angles were evaluated relative to the optical axis, and then 5° was added to the input ray angles to account for the average foveola location. The Zemax raytrace software does not have standard methods that facilitate this type of evaluation, but additional capabilities were created for the modeling, and ultimately ray intersections with the retina were saved to a file and exported to Matlab (Mathworks, Natick MA) for separate evaluation. The following methods were used. (a) Special optical surfaces were created for both IOL surfaces using the “user defined surface” capability, so that both the rays passing through the IOL and rays missing the IOL were recorded with a “sequential” raytrace. Without this, all rays that miss the IOL are stopped. Earlier work had run two separate raytraces^{3,17}, but that prevented the rays reaching the edge of the IOL from being visible in a single plot. Any rays that hit the outer edge of the IOL were ignored, which simulates the effect of a rounded and frosted lens edge that widely scatters the light over a large region. (b) The model eye was set up so that it could be rotated about a vertical axis, and a Zemax macro was used to record the coordinates of ray intersections with the retina for object points at a 6 meter distance. The macro takes advantage of the “ray aiming” capability of Zemax to find the location of the iris boundary for rays from each object point, and then launches a set of rays that are equally spaced in angle. A separate “polarization” routine was used to calculate the fraction of each refracted light ray that reached the retina, after Fresnel reflections were removed, and this was also saved. Both rays that pass through the IOL, and rays that miss the IOL, form part of the set of rays. (c) The retinal ray intersections were then imported into Matlab (Mathworks, Natick, MA) for analysis and display.

For most of the evaluations here, the retinal locations were scaled directly to object space using the angle subtended at the second nodal point of the pseudophakic eye (Figure 2). This is

based on that angle being virtually identical to the input angle to beyond 70° for the chief ray passing through the center of the pupil^{3,15,18}. This highly linear relationship starts to change at larger angles, but it is not known how accurate this is, and earlier publications have used the linear relationship for all angles in order to provide relative values^{3,15,18}. Aberrations will also alter the effective ray location for large angles for the light passing through the IOL. The use of the subtended angles permits the retinal image to be displayed as though it were on a quasi-polar plot, in a similar manner to the way visual field results might be considered. This has been found to be very beneficial, because it flattens out the image onto a plane surface for review, while also inverting the image. An input object that consists of a text chart is used for the first time in the analysis here, and this scaling method enables the input object and the resulting image to be compared.

The ray intensities also need to be weighted in order to approximate what a person might see. One adjustment comes from the total transmission values mentioned earlier. Another weighting factor attempts to compensate for the visual effect of a reduction in image intensity at very large angles because the pupil effect becomes increasingly elliptical with increasing visual angle, resulting in the horizontal pupil opening getting progressively smaller. This has an effect on the transmitting area which falls off as an approximate cosine function¹⁵. The mechanism by which the eye compensates for the image getting dimmer in the periphery does not appear to have been researched¹⁷, and to counteract it each ray was weighted by $1/(\cos(0.8 \cdot \text{retinal angle}))$. A “gamma correction” value of 0.5 was also used to enhance the visibility of lower intensity levels when they are displayed as an image. After each image was created, by adding weighted rays into a matrix of image points corresponding to horizontal and vertical visual angles, the overall intensity of each image was rescaled again to fill the full intensity range.

In addition to the rays being weighted appropriately, simulated images of a text chart were also created (Figure 3). The point spread function (PSF), which is the image of a point source, varies strongly with radial location, and this is illustrated in Figure 4(b) for a very sparse set of object points in the horizontal direction. Most imaging systems are isoplanatic, where the PSF shows very little variation from point to point, and usually Fourier transform methods are used to generate a simulated image, using a constant PSF. Even where the image is more complex, it can be broken down into sub-regions that are isoplanatic, for calculation. This particular optical system has a highly variable PSF, however, and the image here was generated directly using individual object points. Each ray was weighted by the object intensity, in addition to the other factors, before being added to the final image. Because of the time involved with this, the main images were generated using just the horizontal set of PSF values for all the vertical points in the image, because the changes to the PSF were very modest for the other locations. The images are all monochromatic.

Separately, an exploration was undertaken to see if the angular scaling could be improved, and a phakic eye model for a 70 year old eye was created with a gradient index lens. Earlier evaluations of the scaling for a phakic eye had used a gradient index lens in a widely used model for a young eye³, even though the model had not been created for use at large angles. There are several other phakic eye models in the literature, but even when they are described as being “wide-angle” models for the eye, they are typically only used up to perhaps 40° . None of the earlier work seems to go even to 70° , let alone to the limit of temporal vision that is generally assumed to be approaching 110° . The limiting visual angle also appears to have seen little research. In particular, the variation with age does not appear to be known, and it is not clear how large the limiting visual angle is for a phakic 70 year old eye. The modeling here used a

user-defined surface from Akram¹⁹, based on work by Bahrami²⁰, and it was further modified to have an aspheric anterior surface (Fig 5). A 70 year old eye was modeled^{21,22}, and the chief ray was evaluated with increasing angle. This largely verified the earlier simpler calculations, with a linear relationship to very large input angles, followed by a droop in the curve. This new scaling was then used to generate images comparing the phakic and pseudophakic eyes directly, this time using the actual calculated PSF values for each horizontal and vertical object point.

Sketches were also created illustrating the characteristics of “positive” dysphotopsia²³, using a polar plot representing object space, to assist with the discussion section.

RESULTS

The main simulated image in the periphery from this calculation method for a 2.5 mm diameter pupil is given in Figure 6. At a very large angle, the main image that is formed by the IOL becomes dark, which is where the vignetting is so prominent that it truncates the focused image. Light can also miss the IOL, however, and that creates the additional image region further out, with a dark region in-between that would appear as a shadow. This image also illustrates an additional characteristic of the overall optical system, however, because the outer image actually comes from a lower visual angle, and part of the object is actually seen twice. This information is already included in raytrace plots like the depiction in Figure 2, where a single input ray is split at the edge of the IOL, but the text image characterizes this in a clearer manner. It can also be seen that the outer region is larger because it has not experienced the additional power of the IOL, and also that the two regions have different aberrations. Text would not normally be clearly

resolved at these very large angles, but the overall optical effects are illustrated by these imaging simulations.

Additional characteristics are depicted in Figure 7, where in Figure 7(a) the eye rotates about a vertical axis. It can be seen that the K and D move from the outer region to the central region as the eye rotates, but the dark shadow stays in the same place. With the eye steady, and the pupil opening, however, the shadow is rapidly dissipated with very small pupil diameter changes (Figure 7(b)).

Figure 8 gives images that compare a phakic and pseudophakic 70 year old eye, using the revised scaling that is not linear at very large visual angles, and where each object point is used with its own PSF (rather than using the horizontal PSFs for all image locations). This indicates that the total limit for the image of the phakic eye is about 105° , which is in agreement with general thinking about the eye, though it is not clear that there are any published values at all for the older eye. With the pseudophakic eye, the magnification is slightly different, because although the IOL power is chosen so that the image is in focus on the retina, the effective axial location where the IOL power has an effect is different to that of the phakic eye. The main focused image only extends to about 95° because the light is vignetted at the IOL. The displayed image is extended out to 120° here in order to make the “D” clearly visible, though presumably vision does not normally extend to this angle. This is really scaling of the retina as though the eye was a phakic eye, and details of the retinal behavior in this region are not really known.

Figure 9 adds additional schematic images related to positive dysphotopsia, using the framework of a polar plot in object space that was introduced above. This is used in a discussion later about what might be “bothersome” for a patient experiencing negative dysphotopsia, and although there are general discussions about this in the literature, it is not clear that the motion

characteristics of the image are fully described anywhere. Positive dysphotopsia, which is characterized by an arc or flash of light near the fovea, is seen with a large pupil at night (in comparison to negative dysphotopsia, which is seen with a small pupil under bright illumination). In Figure 9 (center), if there is only a single point light source at about 30 degrees of visual angle, and the IOL has a perfectly cylindrical outer edge, raytracing indicates that all the light that hits the edge near the horizontal will be totally internally reflected in the general direction of the fovea. The illuminated region looks like an arc. If the eye rotates to look at the light (Figure 9 (Left)), the light does not hit the lens edge so there is no secondary image. If the eye rotates the other way, an arc of light will suddenly appear near the fovea when light starts to be reflected from the edge, but it appears to move away from the rotating eye because it is being seen in reflection, and it moves at twice the speed of the eye rotation. Also, as the angle increases, more of the edge is receiving the incident beam as it moves toward more normal incidence on the edge within the lens. However, light also gets increasingly transmitted through the edge rather than being reflected when it is beyond the critical angle, and the image rapidly disappears.

DISCUSSION

Text is never resolved clearly in the far periphery, but the simulated text images that have been calculated here provide clarification about what happens to light reaching the retina in this visual region. With a small pupil, the main focused image can go totally dark at large visual angles, and this is very likely to be the primary cause of negative dysphotopsia. However, rather than being an unexpected artifact caused by specific IOLs, or surgical techniques, it is a fundamental property of the pseudophakic eye. This visual region has never really been evaluated as an imaging system before, for either phakic or pseudophakic eyes, because patients typically do not

complain about vision in the far periphery, and it is not a specific field of study. Even if nobody was complaining about “dark shadows” in the periphery, the analysis raises questions about what is actually seen there. The topic has arisen because of intraocular lenses, but similar questions apply to the phakic eye.

. The initial raytrace modeling showed where the light rays went ³, this was extended later to illustrate peripheral retinal illumination with an extended source ¹⁵, and the simulated text charts included here now provide additional clarification (Fig 7). The images show that the shadow can be very prominent with small pupils, but that it rapidly gets fainter as the pupil opens up and the peripheral retina is flooded with light that misses the IOL. This is consistent with the general clinical understanding about negative dysphotopsia ^{6,10,24}, where it is most noticeable with small pupils. The text images also show that the first letter in the region beyond the shadow is the same as the last letter in the primary image, so the object is being seen twice. This is the same type of information that the bifurcated beam provides in raytrace drawings (Fig 2), but it is easier to visualize. The evaluations demonstrate a clear mechanism for how a shadow is created in the periphery, though at the moment there is not enough detail in clinical reports of negative dysphotopsia to definitively confirm the cause (and there may also be other shadowlike phenomena that have different causes).

One particular difficulty with raytrace modeling is the scaling of the images. This is partly because the pseudophakic eye can have a double image in the periphery, but also because the retina is highly curved, and the physical location of image regions is not usually mapped back to visual angles. The image location on the retina has to be related back to what is *perceived* to be the corresponding visual angle. Using linear scaling extrapolated from lower angles ³, the raytrace modeling indicates that the shadow is at large angles of 80-90 degrees, but the angle is

not exactly known. A new attempt here to model the older phakic eye indicates that there is a non-linearity at larger visual angles, but there appear to be no studies that have evaluated this relationship.

The peripheral double image is also a particular problem for perimetry, where the patient responds only that they have seen a stimulus, and not where that stimulus was seen. The pupil diameter is also typically not controlled, or even measured, during perimetry, and even for perimetry studies related to dark shadows, no pupil diameters are provided. There are now several reports of differences in perimetry for patients who see dark shadows, but it is not clear how closely the features that are measured correspond to the shadows that the patient perceives to be bothersome^{5,25,26}. One difference between patients is also the lens style that is used, and in many studies the lenses are evaluated as a single group. However, it has recently been noted that IOLs with a lower refractive index typically have a reduced optical diameter on one or both surfaces¹⁸, and differences like this may affect image luminance at different angles.

The actual situation is probably that there are nuances in the overall visual field of the pseudophakic eye that have just never been explored before, and these probably vary with pupil diameter and lens style. A recent paper reports that most patients with ND feel that the ND-shadow is far in the periphery⁸, but additional shadowlike effects are also recorded for those patients at much lower visual angles. The incidence of ND reports in that study is about 1.3%. At the recent symposium on Negative Dysphotopsia at the ESCRS in Paris, 2019, it was also reported that shadows were measured objectively for patients for many different visual angles (“Quantifying negative dysphotopsia”, S. Palkovits). The specific cause of these shadows was not modeled, but this must be a different type of shadow to the vignetting described here at large angles.

The various evaluations and discussions in the main references about negative dysphotopsia indicate that the bothersome shadows are only seen with small pupils. The calculations here can be used with that information to actually define a very clear hypothesis for the primary cause of dark shadows in the far periphery. The hypothesis might be stated as follows: *At very large visual angles light cannot pass through the IOL when the pupil is small, and the main image goes dark.* There do not appear to be standard measurement methods that can be used to evaluate this hypothesis, because this visual region is usually measured only with perimetry, which is generally set up so that the effects of things like refractive error and pupil diameter do not affect the results. What is really needed is a test where the patient actually sees a shadow, and the visual angles relating to it are recorded, along with the pupil diameter. The lack of control over pupil diameter is a particular problem with conventional testing.

A description of “positive dysphotopsia” has also been included here, because lens edge reflections are known to be “bothersome”, and the use of an input visual angle plot provides a new format for discussing the characteristics. There are various discussions in the literature about this topic, but little that actually fully describes what might make this very annoying for a patient. The discussion in the Results section relating to Figure 9 indicates that light entering the eye at modest visual angles (for example at about 30 degrees) can reflect an arc of light near the fovea, and that this arc can seem to appear and disappear as the eye moves. The bright arc does not appear to be linked to any light source that is in the visual field, and the patient is not normally able to fixate on it. This is probably what makes it particularly bothersome, though evaluations of positive dysphotopsia have not typically related detailed laboratory measurements of specific IOL styles to clinical observations. Discussions have been of a more general nature, without stating a clear hypothesis that was evaluated in detail.

A similar situation exists now for negative dysphotopsia, where it is known that peripheral shadows are a problem, but it has not been explained why they are “bothersome”. Vision in the far periphery is particularly sensitive to motion, and the raytrace calculations indicate two potential mechanisms that may attract attention to the region of the shadow. One possibility is that a very small change in pupil diameter can cause a very large change in the darkness of the shadow, and if the pupil changes rapidly it may be perceived as being movement in the periphery. A second possibility is that because the light that misses the IOL has a different magnification to the primary image, with the image detail appearing twice, that may also lead to a sense of unusual motion in the far periphery. These two mechanisms may also combine, because the eye and the iris are typically always moving, and the patient may also move physically through an environment that has strong visual stimuli. In comparison, the eye is never bothered by the blind spot created by the optic nerve, even though this is always in the same location on the retina, in a similar manner to the dark shadow being primarily at a fixed location. However, the retinal region near the blind spot never sees at all, but the peripheral retina region evaluated here is always sensitive, and for larger pupil diameters it is always illuminated. There are no publications that specifically mention effects like these, but a second part of the hypothesis might be: *“Light missing the IOL illuminates the peripheral retina directly, creating the appearance of a shadow with small pupils, while also repeating image detail with a different magnification. Rapid changes in pupil diameter, or motion of the eye when there is strong object detail, may lead to a sudden change in the appearance of the visual field in the periphery, making it bothersome for the patient”*.

There are several recent publications that discuss methods for treating negative dysphotopsia, and these include alternative theories for their cause^{2-4,6,24,27}. One treatment method is reverse

optic capture, with discussions also about how the anterior capsule may be involved. This method may also move the IOL closer to the iris, which would be expected to alter the visual phenomena anyway. Another treatment method is to use a secondary piggyback IOL in the sulcus^{26,28}, which is thought to be 70% effective. A raytrace evaluation of thick silicone piggyback lenses found that the iris was moved forward, which altered the shadow, though this was only effective in 2 out of 3 patients¹⁶. Other piggyback lenses are thinner, but alleviation of ND symptoms was similar²⁶. The haptic orientation may also have an effect²⁹, and neuroadaptation, and the effect of the second eye, have also been considered to affect the perception of ND²⁷.

The raytrace modeling also raises questions about the total field of view of the pseudophakic eye, and there do not appear to have been any evaluations of this. It has probably always been assumed that a patient with an IOL sees things in a similar manner to a phakic person, but just a glance at Figure 1 would question this. However, IOL surgery developed over a period of decades without the benefit of images like this, and patients never really complained. The raytrace calculations indicate that the limiting field of view is smaller when the pupil is small. The evaluation here only considers a specific eye, and there are large variations in eye parameters across the population, so there may be a large number of expected outcomes due to variations in such things as corneal power, axial length, pupil diameter, IOL centration, IOL style, and the separation between the iris and the IOL.

Overall, the earlier publications, and the more recent raytrace evaluations, support a single theory about negative dysphotopsia in the far periphery. Both the thickness and diameter of the IOL are very much smaller than the same dimensions for a crystalline lens. With a small pupil, the main image is no longer focused by the IOL, and it goes dark at large angles. Light can also miss the

IOL, and this can provide illumination to the far peripheral retina, but this does not come from visual angles that correspond with phakic vision. The combination of these effects can lead to a region whose darkness varies dramatically with small pupil diameter changes, with dark regions being perceived as a shadow. Any motion of image detail in the very far periphery will also be different to motion of the more central image because it is not focused by the IOL. A systematic evaluation of all the factors that affect this visual region should be able to confirm the cause.

What was known

- The peripheral image formed by an IOL is limited by the lens diameter with a small pupil, but light missing the IOL can also illuminate more peripherally, leaving a dark shadowlike region.

What this paper adds:

- Simulated images confirm the shadow, and also demonstrate that the peripheral light comes from a lower visual angle, and that it is very sensitive to pupil diameter.
- Far-peripheral imaging with the pseudophakic eye is very different to that of the natural eye, whether or not dark shadows are reported.

Acknowledgements. Grateful thanks to Prof. Nadeem Akram for the Zemax gradient index model¹⁹, and to Maria Muzyka-Woźniak MD for OCT images⁹.

REFERENCES

1. Davison JA. Positive and negative dysphotopsia in patients with acrylic intraocular lenses. *J Cataract Refract Surg.* 2000;26(9):1346-1355.
2. Holladay JT, Zhao H, Reisin CR. Negative dysphotopsia: the enigmatic penumbra. *J Cataract Refract Surg.* 2012;38(7):1251-1265. doi:10.1016/j.jcrs.2012.01.032
3. Holladay JT, Simpson MJ. Negative dysphotopsia: Causes and rationale for prevention and treatment. *J Cataract Refract Surg.* 2017;43(2):263-275.
4. Masket S, Fram NR, Cho A, Park I, Pham D. Surgical management of negative dysphotopsia. *J Cataract Refract Surg.* 2018;44(1):91-97. doi:10.1016/j.jcrs.2017.10.038
5. Makhotkina NY, Berendschot TTJM, Nuijts RMMA. Objective evaluation of negative dysphotopsia with Goldmann kinetic perimetry. *J Cataract Refract Surg.* 2016;42(11):1626-1633. doi:10.1016/j.jcrs.2016.09.016
6. Henderson BA, Geneva II. Negative dysphotopsia: A perfect storm. *J Cataract Refract Surg.* 2015;41(10):2291-2312. doi:10.1016/j.jcrs.2015.09.002
7. Makhotkina NY, Nijkamp MD, Berendschot TTJM, van den Borne B, Nuijts RMMA. Effect of active evaluation on the detection of negative dysphotopsia after sequential cataract surgery : Discrepancy between incidences of unsolicited and solicited complaints. *Acta Ophthalmol.* 2017;(June):1-7. doi:10.1111/aos.13508
8. Wenzel M, Langenbucher A, Eppig T. Causes, Diagnosis and Therapy of Negative Dysphotopsia (In German). 2019:767-776.
9. Simpson MJ, Muzyka-Woźniak M. Iris characteristics affecting far peripheral vision and negative dysphotopsia. *J Cataract Refract Surg.* 2018;44(4):459-465. doi:10.1016/j.jcrs.2018.01.028
10. Vámosi P, Csákány B, Németh J. Intraocular lens exchange in patients with negative dysphotopsia symptoms. *J Cataract Refract Surg.* 2010;36(3):418-424. doi:10.1016/j.jcrs.2009.10.035
11. Pereira FAS, Cronemberger S. Ultrasound biomicroscopic study of anterior segment changes after phacoemulsification and foldable intraocular lens implantation. *Ophthalmology.* 2003;110(9):1799-1806. doi:10.1016/S0161-6420(03)00623-7
12. Simpson MJ. Mini-review: Far peripheral vision. *Vision Res.* 2017;140. doi:10.1016/j.visres.2017.08.001
13. Coroneo M, Pham T, Kwok L. Off-axis edge glare in pseudophakic dysphotopsia. *J Cataract Refract Surg.* 2003;29(10):1969-1973.
14. Hong X, Liu Y, Karakelle M, Masket S, Fram NR. Ray-tracing optical modeling of negative dysphotopsia. *J Biomed Opt.* 2011;16(12):125001-1-7.
15. Simpson MJ. Simulated images of intraocular lens negative dysphotopsia and visual

- phenomena. *J Opt Soc Am A*. 2019;36(4):B44-B51. doi:10.1364/josaa.36.000b44
16. Erie JC, Simpson MJ, Bandhauer MH. Effect of a sulcus-fixated piggyback IOL on negative dysphotopsia: A ray-trace analysis. *J Cataract Refract Surg*. 2018:Submitted.
 17. Simpson MJ. Mini-review: Far peripheral vision. Vision Research. *Vision Res*. 2017;140:96-105.
 18. Erie JC, Simpson MJ, Bandhauer MH. Effect of a sulcus-fixated piggyback intraocular lens on negative dysphotopsia: Ray-tracing analysis. *J Cataract Refract Surg*. 2019;45(4):443-450. doi:10.1016/j.jcrs.2018.10.041
 19. Akram MNA, Baraas RC, Baskaran K. A wide-field emmetropic human eye model based on ocular wavefront measurements and geometry-independent gradient index lens. *J Opt Soc Am A*. 2018;35(11):1954-1967. doi:10.1364/JOSAA.35.001954
 20. Bahrami M, Goncharov A V. Geometry-invariant GRIN lens: finite ray tracing. *Opt Express*. 2014;22(23):27797-27810. doi:10.1364/oe.22.027797
 21. Moffat B., Atchison DA, Pope J. Age-related changes in refractive index distribution and power of the human lens as measured by magnetic resonance micro-imaging in vitro. *Vision Res*. 2002;42(13):1683-1693. doi:10.1016/S0042-6989(02)00078-0
 22. Atchison DA, Markwell EL, Pope JM, Swann PG. Age-related changes in optical and biometric characteristics of emmetropic eyes. *J Vis*. 2008;8:1-20. doi:10.1167/8.4.29.Introduction
 23. Holladay JT, Lang A, Portney V. Analysis of edge glare phenomena in intraocular lens edge designs. *J Cataract Refract Surg*. 1999;25(6):748-752. doi:10.1016/S0886-3350(99)00038-3
 24. Masket S, Fram N. Etiology of negative dysphotopsia. *J Cataract Refract Surg*. 2013;39(3):485-486. doi:10.1016/j.jcrs.2013.01.006
 25. Makhotkina NY, Berendschot TTJM, Beckers HJM, Nuijts RMMA. Treatment of negative dysphotopsia with supplementary implantation of a sulcus-fixated intraocular lens. *Graefe's Arch Clin Exp Ophthalmol*. 2015;253(6):973-977. doi:10.1007/s00417-015-3029-8
 26. Makhotkina NY, Dugrain V, Purchase D, Berendschot TTJM, Nuijts RMMA. Effect of supplementary implantation of a sulcus-fixated intraocular lens in patients with negative dysphotopsia. *J Cataract Refract Surg*. 2018;44(2):209-218. doi:10.1016/j.jcrs.2017.11.013
 27. Masket S, Rupnik Z, Fram NR. Neuroadaptive changes in negative dysphotopsia during contralateral eye occlusion. *J Cataract Refract Surg*. 2019;45(2):242-243. doi:10.1016/j.jcrs.2018.12.010
 28. Masket S, Fram NR. Sulcus-fixated IOLs for Negative Dysphotopsia. *J Cataract Refract Surg*. 2015;41(2):478. doi:10.1016/j.jcrs.2014.12.040
 29. Erie JC, Simpson MJ, Bandhauer MH. Influence of the intraocular lens optic-haptic

junction on illumination of the peripheral retina and negative dysphotopsia. *J Cataract Refract Surg.* 2019;1-5. doi:10.1016/j.jcrs.2019.04.019

Figure Legends

Figure 1. Overlay of preoperative and postoperative OCT images for the same eye. Crystalline lens profile estimated using published data ²².

Figure 2. Input visual angles related to retinal location, and displayed approximately on a polar plot. The input visual angle is linearly related to the angle subtended at the 2nd nodal point of the eye up to very large angles.

Figure 3. Approximate location of illuminated peripheral text object displayed on polar plot.

Figure 4. Point spread function images for a few widely-spaced object points using linear scaling for a phakic and a pseudophakic eye. With the pseudophakic eye, light that misses the IOL creates a separate arc as part of the PSF.

Figure 5. Raytrace of 70 year old phakic eye with gradient index lens. The axial and radial refractive index values are sketched in the inset.

Figure 6. Simulated peripheral image.

Figure 7. (a) The effect of rotating the eye with a 2.5mm pupil. (b) The effect of increasing the pupil diameter.

Figure 8. Comparison between images for phakic and pseudophakic 70 years old eyes, using scaling for the phakic eye relative to the 2nd nodal point for both eyes,

Figure 9. Schematic representation of positive dysphotopsia with an IOL.

JCRS figures and captions 2019

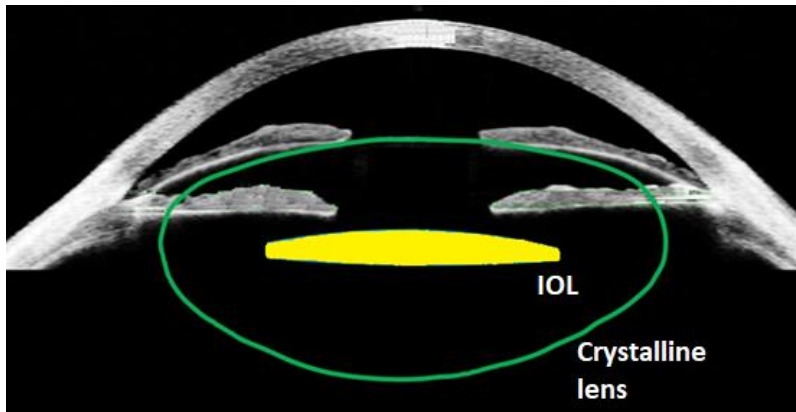


Figure 1. Overlay of preoperative and postoperative OCT images for the same eye. Crystalline lens profile estimated using published data.

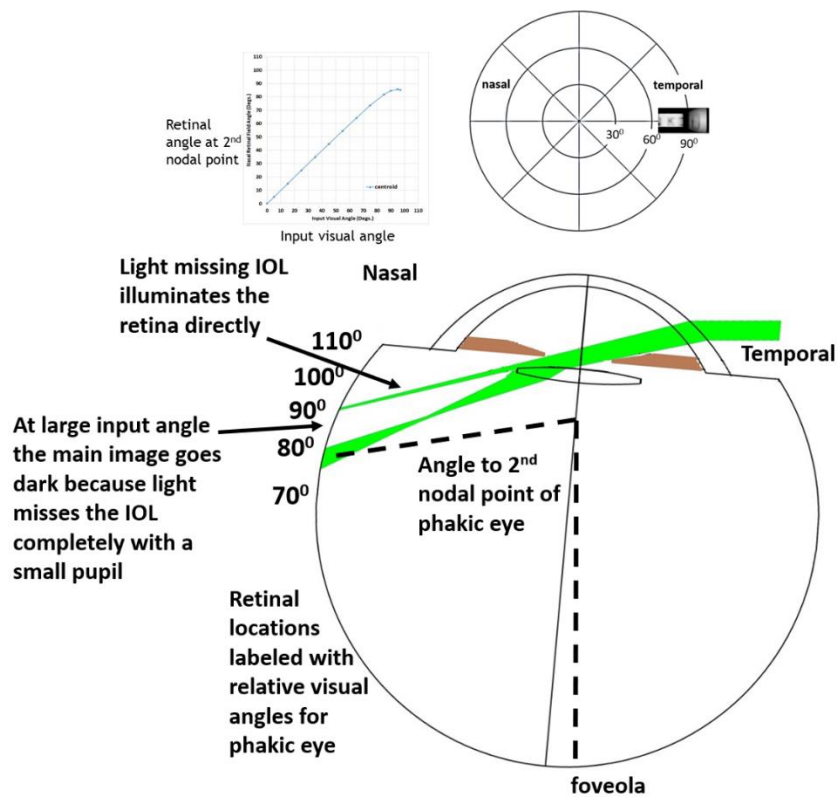


Figure 2. Input visual angles related to retinal location, and displayed approximately on a polar plot. The primary angular relationship is linear, for simplicity.

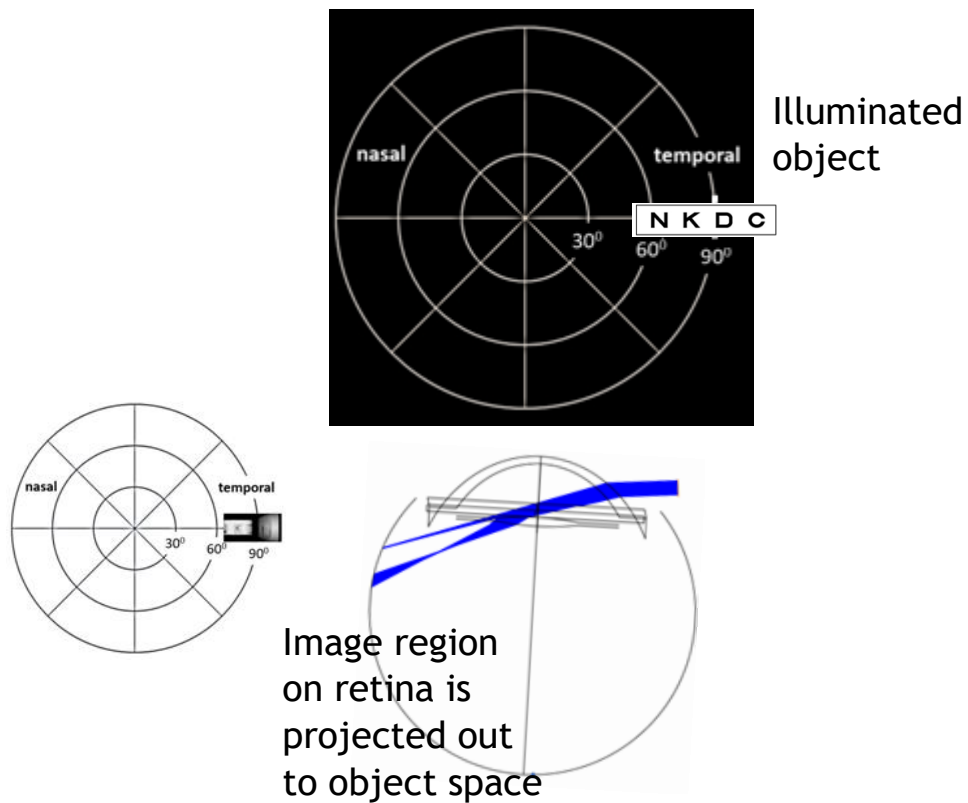


Figure 3. Approximate location of illuminated peripheral text object displayed on polar plot.

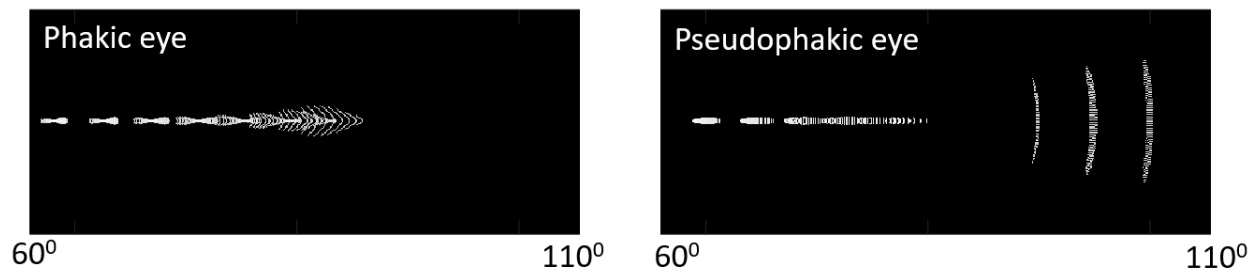


Figure 4. Point spread function images for separate object points using linear scaling for (a) phakic and (b) pseudophakic eyes. With the pseudophakic eye, light that misses the IOL creates the separate arc.

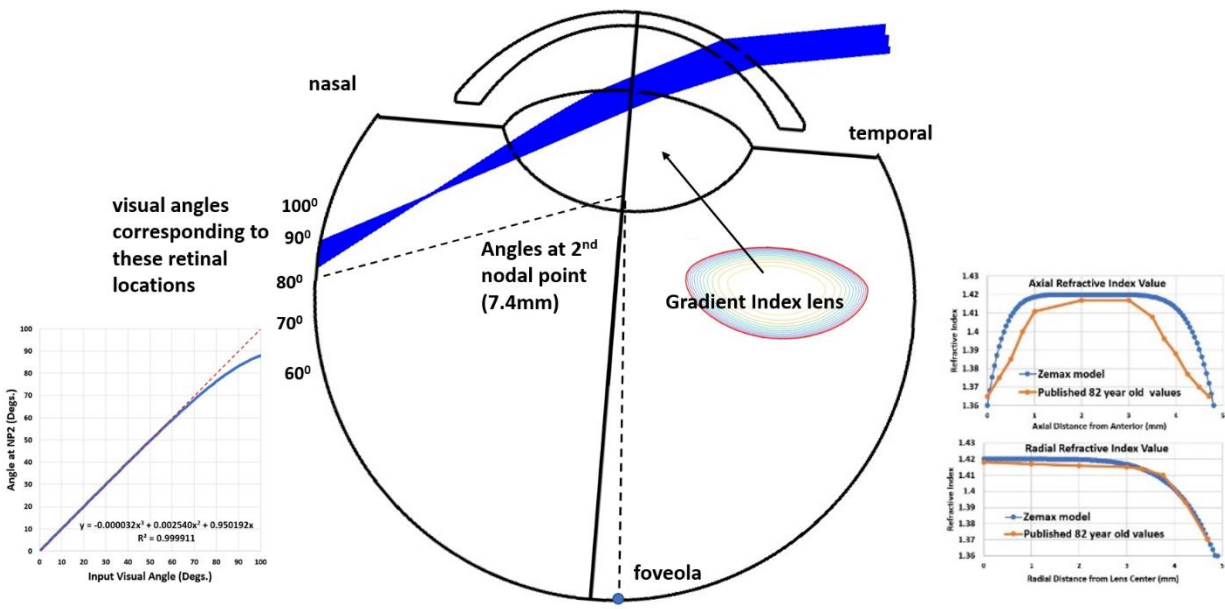


Figure 5. Raytrace of 70 year old phakic eye with gradient index lens. The axial and radial refractive index values are sketched in the inset.

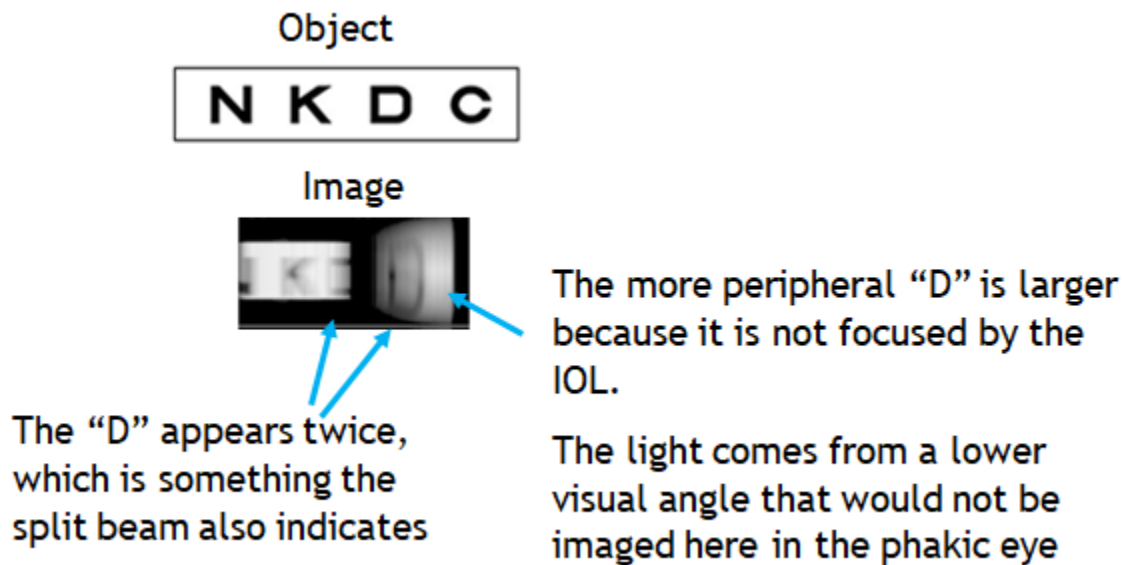


Figure 6. Simulated peripheral image.

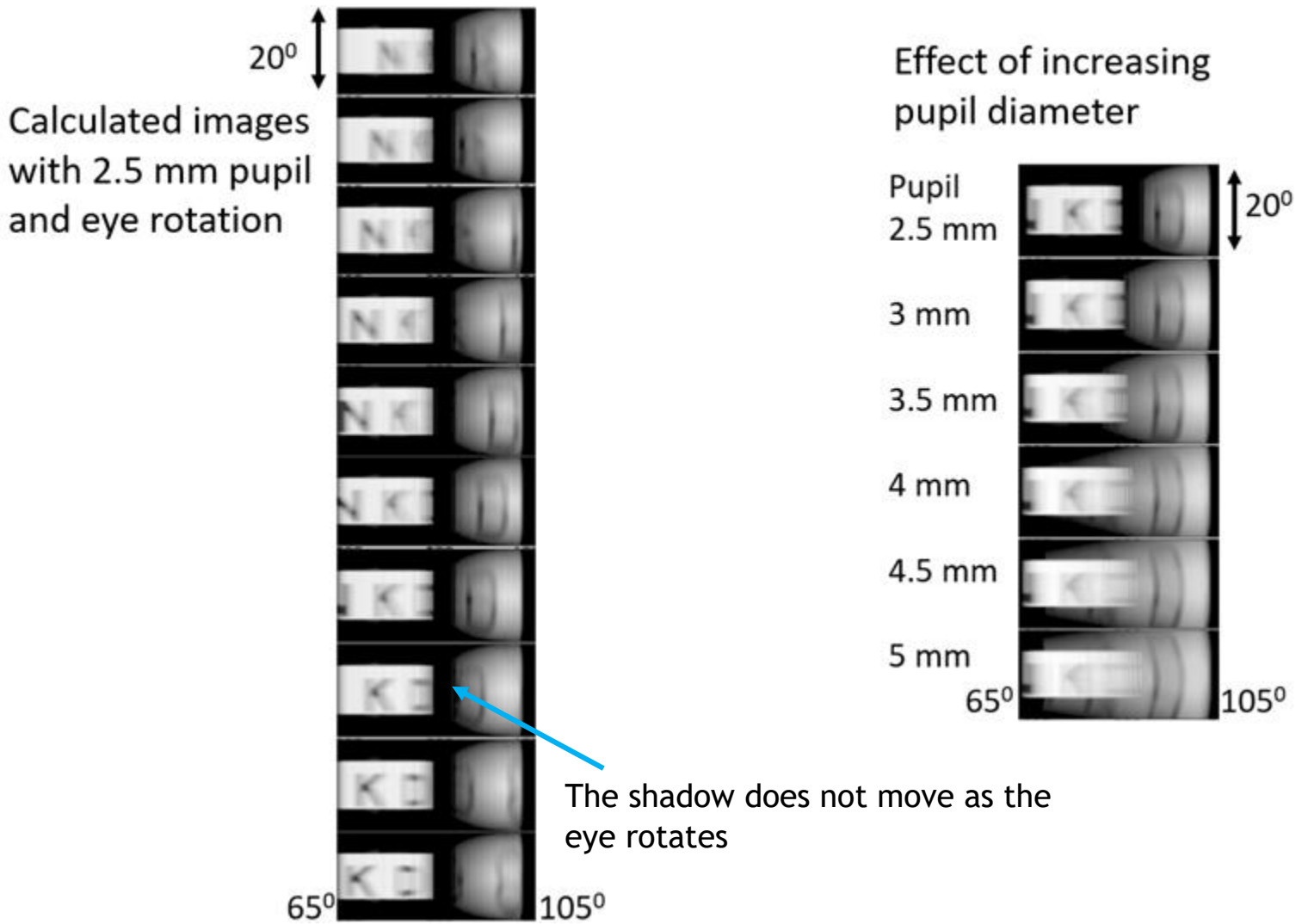
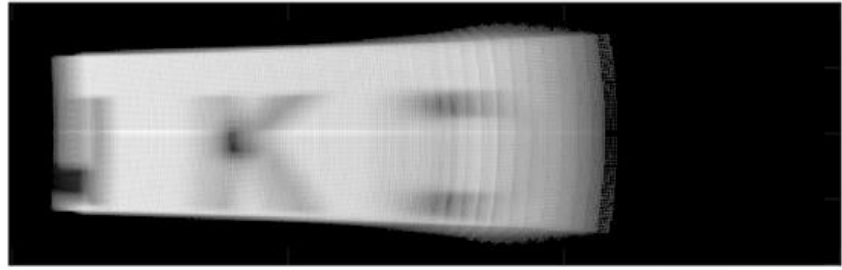
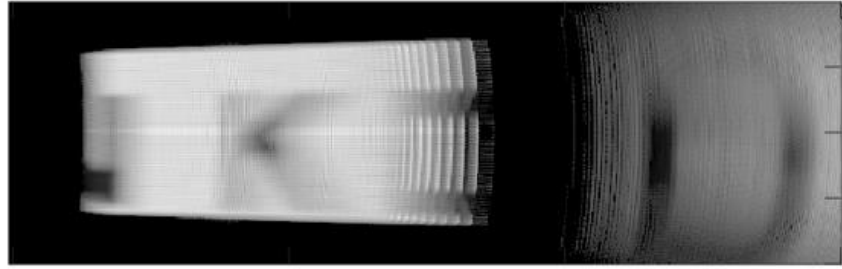


Figure 7. (a) The effect of rotating the eye with a 2.5mm pupil. (b) The effect of increasing the pupil diameter.

70 year old
phakic eye



Pseudophakic
eye



60° 70° 80° 90° 100° 110° 120°

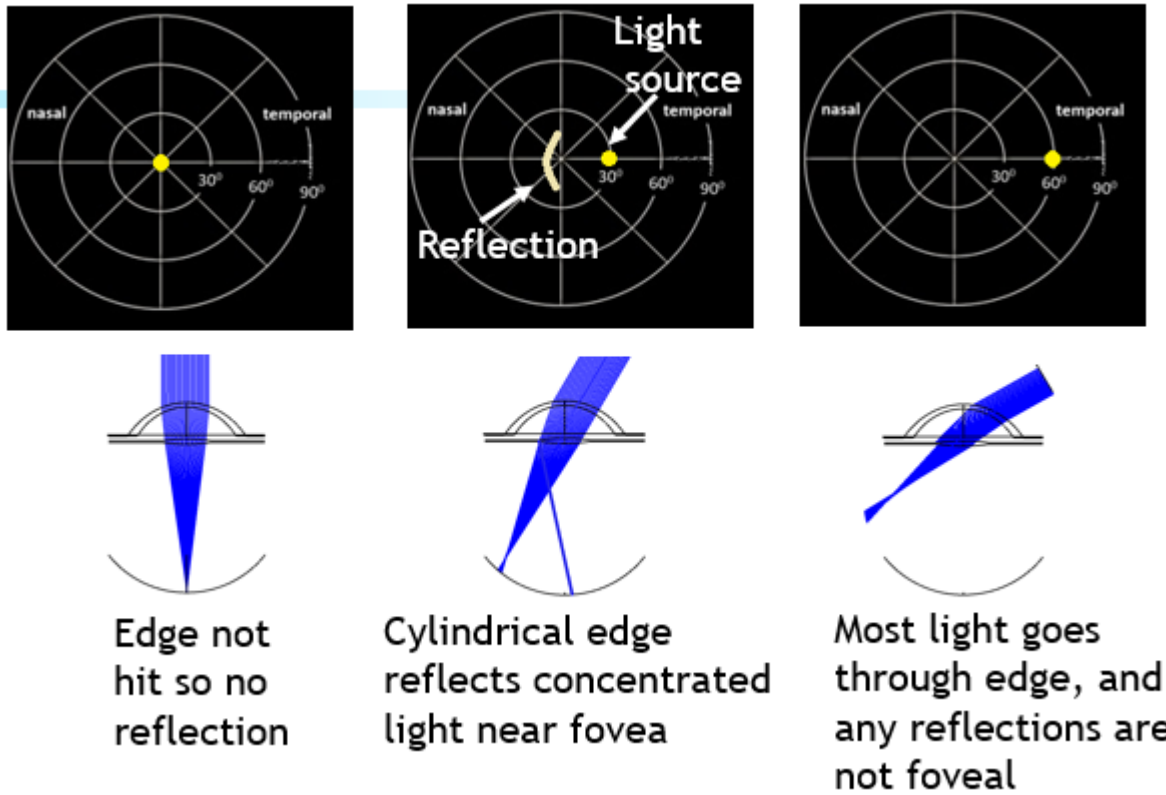


Figure 9. Schematic representation of positive dysphotopsias with an IOL.